Journal of Molecular Graphics and Modelling 38 (2012) 40–49

Contents lists available at SciVerse ScienceDirect

Journal of Molecular Graphics and Modelling

journal homepage: www.elsevier.com/locate/JMGM

Phase transition study of confined water molecules inside carbon nanotubes: Hierarchical multiscale method from molecular dynamics simulation to ab initio calculation

Soheila Javadian[a,*], Fariba Taghavi[a], Faramarz Yari[b], Seyed Majid Hashemianzadeh[c,**]

[a] Department of Physical Chemistry, Tarbiat Modares University, P.O. Box 14115-117, Tehran, Iran
[b] Department of Biology, Science and Research Branch, Islamic Azad University, Tehran, Iran
[c] Molecular Simulation Research Laboratory, Department of Chemistry, Iran University of Science and Technology, Tehran, Iran

ARTICLE INFO

Article history:
Received 4 February 2012
Received in revised form 3 May 2012
Accepted 5 May 2012
Available online 9 June 2012

Keywords:
Confined water
Ice nanotubes (ice NTs)
Phase transition
Molecular dynamics (MD) simulation
Natural bond orbital (NBO)
Nuclear quadrupole resonance (NQR)

ABSTRACT

In this study, the mechanism of the temperature-dependent phase transition of confined water inside a (9,9) single-walled carbon nanotube (SWCNT) was studied using the hierarchical multi-scale modeling techniques of molecular dynamics (MD) and density functional theory (DFT).

The MD calculations verify the formation of hexagonal ice nanotubes at the phase transition temperature T_c = 275 K by a sharp change in the location of the oxygen atoms inside the SWCNT. Natural bond orbital (NBO) analysis provides evidence of considerable intermolecular charge transfer during the phase transition and verifies that the ice nanotube contains two different forms of hydrogen bonding due to confinement. Nuclear quadrupole resonance (NQR) and nuclear magnetic resonance (NMR) analyses were used to demonstrate the fundamental influence of intermolecular hydrogen bonding interactions on the formation and electronic structure of ice nanotubes. In addition, the NQR analysis revealed that the rearrangement of nano-confined water molecules during the phase transition could be detected directly by the orientation of ^{17}O atom EFG tensor components related to the molecular frame axes. The effects of nanoscale confinements in ice nanotubes and water clusters were analyzed by experimentally observable NMR and NQR parameters. These findings showed a close relationship between the phase behavior and orientation of the electronic structure in nanoscale structures and demonstrate the usefulness of NBO and NQR parameters for detecting phase transition phenomena in nanoscale confining environments.

1. Introduction

From an application standpoint, increasing our understanding of the behaviors of nanoscopic confinement systems is important for designing new molecular devices in physics, chemistry, biology and material science [1]. The essential roles of water in nature and the unique properties of water have motivated numerous investigations to find the anomalous properties of water that is confined in nanometer porous environments [2,3].

Single-wall carbon nanotubes (SWCNTs) are the most favored material in nanotechnology because of their structural stability, low reactivity and unique electric and mechanical properties. These structures have motivated the use of water-filled SWCNTs as an ideal model for studying confined nano-fluid systems [4,5]. The behaviors of water inside and outside a nanoscopic pore are completely different from those of bulk liquid water [6–11]. To determine how the properties of water depend on nanoscale confinement, the structural and thermodynamic properties of water in the nanoscale hollow interior of SWCNTs have been investigated in many recent theoretical [4,5,12–14] and experimental studies, including those that used natural scattering [15], IR spectroscopy [16], Raman spectroscopy [17] and X-ray diffraction (XRD) [18]. These studies have shown that the effects of confining surfaces are strongly related to the diameter of a carbon nanotube. The properties of water in tubes with diameters larger than 25 Å are very similar to those of bulk water. However, when the CNTs are narrower, certain properties, including the hydrogen bond network and self-diffusion coefficient, differ significantly from those of bulk water [5].

An understanding of the unexpected phase behaviors of systems under confinement facilitates the development of innovative applications such as nanopower harvesting devices [19] and ferroelectric nano devices [14]. Confined water in a carbon nanotube could be an ideal model for studying the anomalous phase behaviors of confined systems. In 2001, Koga et al. used a computation method to determine that water can exhibit a first-order phase transition to

* Corresponding author. Fax: +98 21 82883455.
** Corresponding author.
E-mail addresses: javadian_s@modares.ac.ir, javadians@yahoo.com (S. Javadian), hashemianzadeh@yahoo.com (S.M. Hashemianzadeh).

1093-3263/$ – see front matter © 2012 Elsevier Inc. All rights reserved.
http://dx.doi.org/10.1016/j.jmgm.2012.05.009

n-gonal ice nanotubes (ice NTs) [20]. Following that study, there has been a great deal of interest in simulating the properties of freezing water inside carbon nanotubes [12,21–25]. Although there have been widespread reports on this subject, the simulation results were not all in agreement, particularly with respect to the choice of Lennard–Jones parameters, the method of calculating long-range forces and the water molecular models such as SPC/E or TIP3P [26]. However, all of the simulation studies revealed the possible existence of a new water phase inside SCNTs at temperatures below room temperature.

Experimental investigations have shown that there is an ordered structure of water in carbon nanotubes at low temperatures [15,27,28], and it was recently confirmed that water shows a transition from a liquid-like structure to novel ice structures known as ice NTs [14,29]. However, a fundamental understanding of the electronic features of freezing water inside carbon nanotubes remains unclear. In addition, there is no evidence of how the phase transition of water inside SWCNTs as thermodynamic bulk phenomena could be detected through the electronic properties of a water molecule in this system.

In this study, we investigated the electric mechanism of the phase transition in water-filled SWCNTs using density functional theory (DFT) and molecular dynamic (MD) simulations. We discussed how confinement within SWCNT pores affects the electronic configuration and hydrogen bond network of the water structure inside SWCNTs by natural bond orbital (NBO) [30,31], nuclear magnetic resonance (NMR) [32] and nuclear quadrupole resonance (NQR) [33] analyses. Accordingly, the molecular aspects underlying the first-order phase transition of water inside SWCNTs were clarified. We also introduced novel experimental techniques for recognizing this phase transition. In this study, we considered useful approximations to carry out first-principle calculations; interestingly, our results of the phase transition temperature range remained in very good agreement with the experimental data [18]. These results are useful because we can relate the molecular electronic configuration of water molecules inside SWCNTs to the phase transition phenomena.

In the next section, we explain the model that was used in this study and the computational details. In the following sections, MD simulations, natural bond orbital (NBO), nuclear magnetic resonance (NMR) and nuclear quadrupole resonance (NQR) analyses of our system of interest will be presented.

2. Methods

2.1. Simulation model and computational details

We first performed MD simulations for water molecules encapsulated in a (9,9) SWCNT to analyze the first-order phase transition of water in a range of temperatures from 300 K to 200 K.

Then, DFT calculations were carried out for output structures from the MD calculations to provide comprehensive insight into the molecular view of the behavior of confined water molecules inside an (9,9) SWCNT during a first-order phase transition (which could not be followed from empirical simulations). Because of the difficulties of performing DFT calculations for a large system that was investigated by MD simulations, some approximations were used to create a simpler model of the large system for the purpose of performing DFT calculations. This simple model was able to predict the phase transition temperature area correctly, as will be discussed in subsequent sections.

2.1.1. Simulation model

First, classical MD simulations were performed with a DL-POLY Classic molecular simulation package [34]. The MD calculations were carried out for water molecules filling the interior part of an isolated armchair SWCNT (9,9) with a fixed length of 43 Å and diameter of 12.2 Å. The carbon nanotube in the MD simulations is considered to be fixed with respect to the center of the simulation box.

The number of encapsulated water molecules in this (9,9) SWCNT is 83 [14]. The water molecules were considered rigid structures and were described by the potential model SPC/E [35] because this model can correctly predict the phase transition temperature [36]. The SPC/E potential is the sum of the short-range interaction potential of Lennard–Jones centers in the positioning of oxygen atoms and the long-range potential electrostatic potential between the point oxygen and hydrogen atoms on different water molecules [37]:

$$\begin{aligned} V_{WW} &= V_{LJ} + V_{Coulombic} \\ V_{LJ} &= \sum_{i \neq j} 4\varepsilon_{OO} \left[\left(\frac{\sigma_{OO}}{r_{ij}} \right)^{12} - \left(\frac{\sigma_{OO}}{r_{ij}} \right)^{6} \right] \\ V_{Coulombic} &= \sum_{l \neq m} \frac{1}{4\pi\varepsilon_0} \frac{q_l q_m}{r_{lm}} \end{aligned} \quad (1)$$

where the r_{ij} is the oxygen-oxygen distance, σ_{OO} and ε_{OO} are the Lennard–Jones parameters, r_{lm} is the distance between two point charges q_l and q_m in different molecules, and ε_0 is the vacuum permittivity.

The intermolecular interaction potentials between the carbon atoms in the SWCNT and the water molecules inside it were considered a Lennard–Jones (LJ) function and were calculated using the Lorentz–Berthelot combining rule [37]. The LJ parameters were: $\varepsilon_{OO}/k_B = 76.6$ K, $\sigma_{OO} = 3.15061$ Å, $\varepsilon_{OC}/k_B = 46.3$ K, and $\sigma_{OC} = 3.27531$ Å for oxygen–oxygen and oxygen–carbon interactions, respectively, where k_B is the Boltzmann constant [38]. The parameters of the AMBER force field [38] were used for the carbon atoms in a nanotube. The quadrupole interactions were not taken into account in our simulations because they have a minuscule effect on the resultant water structure [39].

Classic molecular simulations were first performed at a high temperature (300 K). The temperature was then decreased stepwise to 200 K with a temperature variation of 5 K at each run. All simulations were performed for a canonical ensemble (NVT) using the velocity Verlet algorithm [37] for the integration of equations of motion. A step time of 0.1 fs was chosen for the simulation because the typical time required for the dipolar reorientation of water molecules inside carbon nanotube has been reported to be in the order of picoseconds [40]. The Brendsen thermostat [41] was coupled to the system to ensure that the average system temperature is maintained close to the requested temperature at each run. Representative structures at 300 K and 200 K are shown in Fig. 1. The cutoff length for van der Waals forces was set to 20 Å, and Coulombic interactions were ignored at 40 Å. To make the simulation results more applicable for finite systems, periodic boundary conditions were not used in the system of confining a constant number of water molecules with a constant volume inside a SWCNT. The heating and cooling processes were performed to evaluate the reliability of equilibration by reproducing the properties of interest. There was no evidence of a sharp deviation in the tendencies of the properties of interest (especially potential energy), with the exception of the phase transition temperature.

2.1.2. Density functional theory computation methods

Despite the outstanding achievements in empirical MD simulation studies [4,5,14], the microscopic mechanism underlying the hydrogen bond network between water molecules encapsulated within SWCNTs during the cooling process remains unclear.

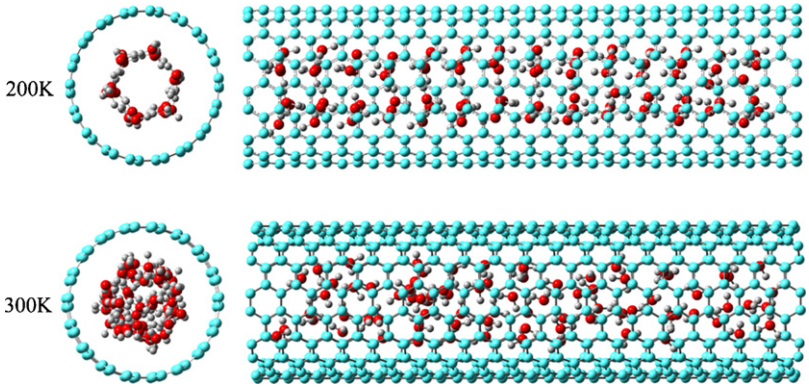

Fig. 1. Snapshot structures of water molecules confined in a (9,9) SWCNT at 200 K (top) and 300 K (bottom). Left: side views. Right: top views. At 200 K, the water structure is composed of a hexagonal ice NT. The small gray spheres and large red spheres represent hydrogen atoms and oxygen atoms, respectively.

Theoretical ab initio calculations represent a promising candidate approach to gain deep insight into the influence of the cooling process on the electronic structure of water at the molecular level. However, this type of calculation cannot include temperature in the geometry optimization. In this study, temperature can be assayed indirectly in ab initio calculations through the use of final configurations that were obtained from MD simulations that contain temperature as initial configurations for the first-principle calculations.

To generate the initial configuration for an ab initio calculation with the help of MD simulations, random sampling was performed on the equilibrium trajectory structures at each temperature. Then, random selected structures were averaged over a time interval to obtain a final configuration for each temperature in a range from 300 K to 200 K [42].

Because of the limitations in satisfying the computational demands for ab initio calculations of the large systems that were studied in the first step via MD simulations, some approximations were made to exchange the system with a smaller and simpler model. We considered the water molecules encapsulated in five rings of carbon atoms in the middle of an armchair SWCNT (9,9) and performed ab initio calculations on the water molecules inside the midsection of the SWCNT. These approximations made the ab initio calculations feasible with our computer facilities.

To carry out the first-principle calculation of the water structures that had been modeled from averaged configurations of MD simulations, DFT [43] was used with B3LYP functional [44,45] and 6-311++G** basis sets in the G098W program package [46,47]. This level of theory was selected because DFT yields accurate solutions in many cases of large structures. Moreover, the hybrid function B3LYP results agree reasonably well with the geometry parameters and physical properties of a water dimer [48]. The NMR and NQR calculations were also performed using the PW91 method (see S3 and S4).

3. Results and discussion

3.1. Molecular dynamics simulations

There have been many reports of MD simulations of water inside SWCNTs [4,14,16,20,49–52], and many of these reports have provided detailed statements about a rapid change in potential energy during the cooling process as evidence of a first-order phase transition [14,16,20,51].

We investigated the phase transition phenomena for 83 water molecules inside a (9,9) SWCNT by decreasing the temperature from 300 K to 200 K via MD simulations. In perfect agreement with a previous study [14], a sudden drop in potential energy at T_c = 275 K was observed as proof of the existence of a phase transition for water at this temperature. Although the use of potential energy is a traditional way to study phase transition phenomena in MD simulations of confined systems, we reported the trends of oxygen atom distributions in the interior of a (9,9) SWCNT with respect to the SWCNT axis as an indication of the transformation from a disordered structure to an ordered structure during the cooling process.

In general, water molecules have more movements in disordered configurations at high temperatures than in ordered configurations at lower temperatures. In addition, the strengthening of hydrogen bonding and the formation of new hydrogen bonds between water molecules during the phase transition make the water molecules more fixed in their local sites by reducing their independent vibrations [16,29]. Thus, studying the oxygen distributions during the phase transition as a dynamic property of water can serve as a method of analyzing the nature of hydrogen bonding during the transformation from a liquid-like state to an ice nanotube. In the current study, the specific geometry of a confined water network inside an SWCNT at each temperature was found to study the behavior of oxygen atom movements around the freezing point temperature of confined water. In addition, configuration information that was obtained here could be used to carry out further studies on the local electron rearrangements around a target oxygen atom by methods such as NBO, NMR and NQR analyses.

The probability of finding an oxygen or hydrogen atom at a specific site Z on the nanotube axis is measured by:

$$n(Z) = \int_{-(L/2)}^{(L/2)} A_{XY}\rho(Z)dZ, \tag{2}$$

where L is the length of the MD cell in the Z direction, A_{XY} is the XY cell area, and $\rho(Z)$ is the mean density at position Z that is defined for all atoms at position z_i by

$$\rho(Z) = \sum_i m_i \Delta(z_i - Z), \tag{3}$$

where m_i is the mass of atom i. In this equation, the $\Delta(z_i - Z)$ function is used to ascribe the position points Z all along the SWCNT axis to atoms as individual central points placed inside an SWCNT [34,53].

The probability of finding an oxygen atom at a certain distance z from the nanotube axis at various temperatures below (200 K and 240 K) and above (285 K and 300 K) the phase transition temperature T_c = 275 K is shown in Fig. 2. $n(Z)$ is given from $Z = [-(L/2), (L/2)]$ where L is the length of the MD cell in this figure.

Fig. 2 shows that the extent of the spatial localization of the oxygen atoms along a (9,9) SWCNT axis is uniform at high

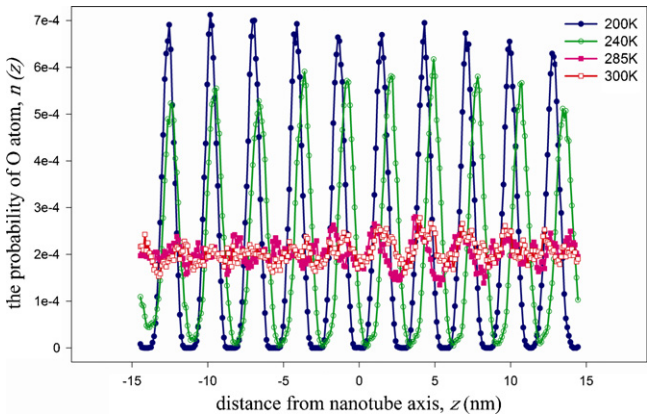

Fig. 2. Radial probability density function for the oxygen atom located at a certain distance z from an SWCNT (9,9) axis at 200 K and 240 K (indicated by filled and open circles, respectively), which are below the phase transition temperature T_c = 275 K, and at 285 K and 300 K (indicated by filled and open squares, respectively), which are above T_c.

temperatures (285 K and 300 K). At low temperatures (240 K and 200 K), this localization suddenly changes to a solid-like distribution, with oxygen atoms placed at defined sites. These findings illustrate a first-order phase transition with a rapid transformation from a disordered structure at high temperatures to an ordered structure at temperatures below 275 K, in agreement with an experimental report [16]. It also should be noted that that most of the oxygen atoms were aligned to C atoms in a bridge position, as shown previously [12]. These findings show that the dynamic movement of confined water inside an SWCNT, as a dynamic behavior of water, could be used to probe the phase transition. From another point of view, the locations of oxygen atoms (water molecules) show extensive changes with temperature variations, which can help to record and define a specific geometry of confined water structure inside an SWCNT.

3.2. NBO analysis

In this study, an NBO analysis provided insight into the electronic nature of an H-bonded network of water molecules encapsulated in an SWCNT. This analysis demonstrated how the nature of hydrogen bonding offers a new mechanism for the electronic and structural reorganization of the phase transition of water inside an SWCNT in the temperature range from 200 K to 300 K.

The NBO analysis was used to reflect the changes in the strength of the hyperconjugation interaction between "filled" (donor) Lewis-type (n) NBOs and "empty" (acceptor) non-Lewis (δ^*) NBOs during the cooling process. The energies of this charge transfer interaction between the chosen water molecule and its neighboring water molecules represent deviations from an ideal Lewis structure and can be calculated by second-order perturbation energies:

$$E_{n\to\delta^*} = -2\frac{\langle n|F|\delta^*\rangle^2}{\varepsilon_{\delta^*} - \varepsilon_n}, \quad (4)$$

where $\langle\delta|F|\delta^*\rangle$ is the off diagonal element of Fock matrix, and ε_n and ε_{δ^*} are the energies of n and δ^* NBOs [30,31].

Fig. 3A depicts a decrease in the donor–acceptor interaction energies $E_{n\to\delta^*}$ involved in an increase in the perturbative delocalization effects for two lone pairs of oxygen atoms as the temperature decreased from 300 K to 200 K. This trend means that the H-bond interactions in the modeled water structure are increased by a cooperative intermolecular charge transfer during the cooling process. Moreover, there is an abrupt drop in the hyperconjugation interaction energies for two lone pairs of oxygen atoms at approximately 275 K, which could be ascribed to a sudden change in the H-bond strength. The results in this figure along with the structural analysis [14] indicates that the sudden change in the H-bond strength could be related to a transformation from a disordered, liquid-like structure at high temperatures to an n-gonal ice nanotube (hexagonal in this case) at low temperatures, which represents a first-order phase transition. Accordingly, the structural configuration of the water molecule network at each temperature was determined by the amount of charge transferred from the donor (n) orbital of the oxygen atom to the acceptor (δ^*) of the hydrogen atom.

In Fig. 3A, there is also a notable difference between the perturbative delocalization energies of the oxygen atom's lone pairs. There is decreased charge transfer energy for a lone pair (1) in the H-bonded network; therefore, as mentioned previously, this lone pair could form a stronger H-bond than the bond of a lone pair (2). The differences in strength of the two hydrogen bonds could be ascribed to the unequal direction of two oxygen atoms' lone pairs with respect to the hexagonal ring in the ice nanotube structure. The lone pair (1) with a lower perturbative energy corresponds to an intra-ring hydrogen bond that is placed in the ring plane, and the oxygen lone pair (2) matches the comparatively weak inter-ring H-bond that is perpendicular to the ring plane. These results are in excellent agreement with experimental vibrational spectroscopy [16] and ab initio [54] studies of hexagonal ice nanotubes. To summarize, we have demonstrated that a convenient approach for characterizing inter- and intra-ring intermolecular H-bonds for a water molecule in a confining geometry is derived from the differences in $n \to \delta^*$ hyperconjugative interaction energies.

Donor–acceptor delocalization interactions also reduce the occupancy of the Lewis orbitals (n in this case) and add it to the vacant non-Lewis NBOs (δ^* here) [30,31]. These donor–acceptor overlaps are estimated here with calculations of charges or populations of the NAO orbital on the atoms of the selected water molecule. As the temperature decreases, the amount of charge transfer increases, which can lead to a decrease in the positive charge on the hydrogen atoms and a simultaneous increase in the negative charge on the oxygen atom (Fig. 3B). Because of the natural charges on hydrogen atoms, at temperatures below 275 K, an intra-ring hydrogen atom has less positive charge than an inter-ring hydrogen atom and therefore has a stronger H-bond due to the larger charge transfer in this direction. These trends are in agreement with observations for two lone pairs of oxygen atoms and, more important, with experimental vibrational spectroscopy studies for the water phase inside SWCNTs [16]. This figure indicates that electron delocalization makes the character of the O—H bond more ionic in the selected water molecule.

As observed previously for perturbative delocalization energies, there is a rapid decrease in the amount of negative charge on the oxygen atom, which is accompanied by a rapid increase in the positive charges on the hydrogen atoms at approximately 275 K. This observation reveals that precipitous structural alterations around the phase transition temperature bring about a change in the electric configuration of confining water molecules.

This significant conclusion could be used to investigate the electronic structure of water-filled SWCNTs. These results show that the electric properties of water molecules encapsulated in SWCNTs at a specific temperature do not all equal that of bulk water. Hence, the unusual arrangement of electrons in confined water molecules influences the dielectric properties of water molecules inside SWCNTs [14]. Equally important, this arrangement could have several consequences for the electrical properties (such as the charge distribution on carbon atoms) [55] and electronic performance (such as voltage generation in water-filled SWCNTs) [19] of water-filled SWCNTs.

Another interesting feature of the hyperconjugative delocalization in H-bonded water confined inside an SWCNT is an increase

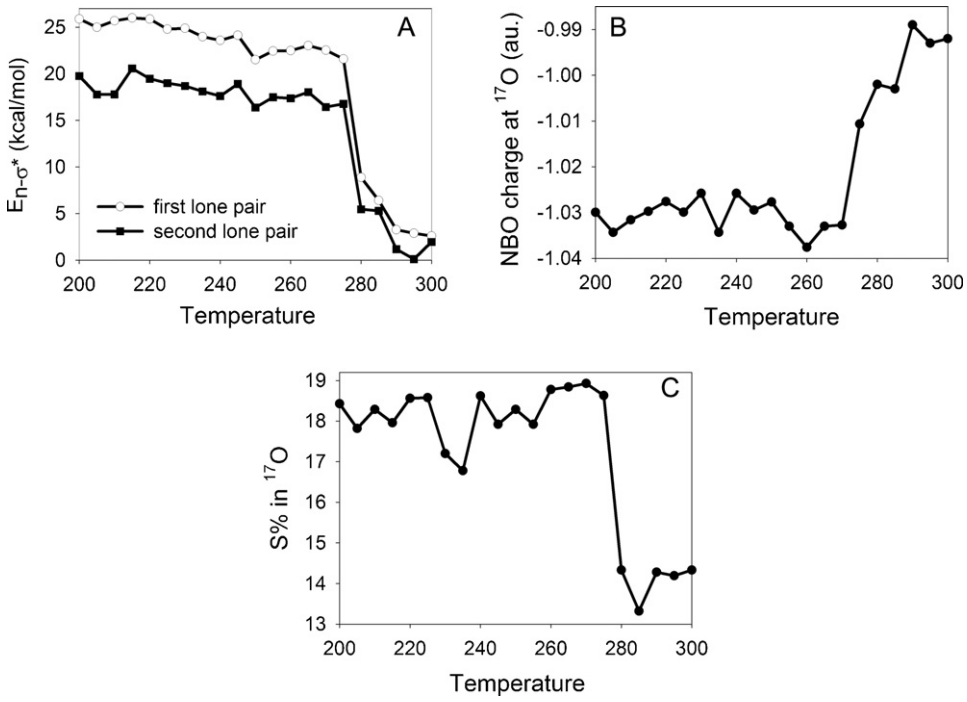

Fig. 3. The temperature dependence of the NBO parameters: (A) energies of the $n \rightarrow \delta^*$ hyperconjugative interactions (kcal/mol) at the B3LYP/6-311++G (2d,2p) level for the first and second lone pairs of the target oxygen atom, represented by open circles and filled squares, respectively. (B) NBO charges (au) of the target oxygen atom. (C) Percent S character (*S*%) of the selected oxygen NAO in the modeled water structure.

in the S character of the oxygen atomic orbital in the O—H bond. This increase has two commensurate results, in agreement with Bent's rule [56]. First, there is an increase in the polarization of the antibonding (δ^*) orbital on the O—H bond in the direction of the H atom, which makes this orbital a better acceptor. Second, there is an increase in the p character of the oxygen orbital (n) to expand its overlap with the antibonding acceptor [30,31]. An appropriate interpretation of the tendency of the percent S character of the selected oxygen NAO in the modeled water structure with respect to temperature (Fig. 3C) is similar to that suggested for the natural charge analysis above. The rapid change in the S character of the natural atomic orbital (NAO) of oxygen atom also occurred at approximately 275 K. Because these NBO calculations could provide useful information about phase transition phenomena, we used NMR/NQR analyses to identify more details about the electronic geometry of confined water.

3.3. NMR–NQR analyses

The local electronic nature of the hydrogen-bonding network in ice nanotubes (ice NTs) could also be described by NMR [57,58] as an atomic size probe on the basis of the inclusion of informative details about local electron density and the H-bonding system of confined water molecules in the chemical shielding tensor of water molecules [59]. In addition, the isotropic part of the NMR chemical shift σ_{iso} does not experience a change in the pure rotation and translation of the molecule and is controlled only by the electron distribution around the nuclei [60]. Therefore, the phase transition in confined water molecules could be traced by the temperature dependence of the isotropic part of the NMR chemical shift σ_{iso} and its sudden change around the phase transition temperature T_c.

In the recent years, information about the phase transition of water confined inside SWCNTs has accumulated through experimental proton NMR techniques, or ^{1}H NMR [29,61–63]. These investigations demonstrated that the confined water inside SWCNTs undergoes a phase transition when the temperature decreases from room temperature to a temperature far below 275 K. By contrast, theoretical ^{1}H NMR studies on water confinement inside SWCNTs are rare [64–66], and no theoretical study has focused on the electronic probing of phase transition phenomena. To our knowledge, there is no theoretical or experimental study on the temperature dependence of ^{17}O NMR parameters for confined water during a phase transition. Moreover, the hydrogen bonding network in ice NTs could be studied with an electric field gradient (EFG) tensor of magnetically active quadrupolar ^{17}O nuclei. There are functional challenges in solid-state NMR experiments of ^{17}O as a quadrupolar nucleus, but a theoretical study of a shielding tensor makes additional details available about the mechanism of hydrogen bonding and its orientation at the phase transition temperature.

In the present study, we report the temperature dependence of a shielding tensor over a temperature range around the phase transition temperature T_c = 275 K. The σ_{iso} shows an obvious anomaly around T_c, which could be ascribed to the electronic structural changes in the mechanism of phase transition phenomena.

In agreement with chemical shielding studies, NQR spectroscopy [33,67,68] is an efficient method for scrutinizing phase transition phenomena of confined water inside SWCNTs.

NQR spectroscopy studies the interaction of the nuclear electric quadrupole moment eQ with an EFG in nuclei with a spin angular momentum I greater than (1/2). The magnitude of this interaction could be measured by the quadrupolar coupling constant C_Q [69]. Additionally, the EFG is a sensor of quantity, and its principal components in the principal axis system (PAS) indicate the magnitude and orientation of an asymmetric electric field caused by a non-homogeneous (asymmetric) electron distribution around the nucleus. The homogeneity of this electric field could be quantified by the asymmetry parameter η of the EFG tensor [59,70]. Furthermore, the orientation of the principal components of the EFG in the molecular frame often correlates with the local electronic configuration [71–73]. Because the formation of ice nanotubes inside SWCNTs is directly related to the nature of hydrogen bonding between water molecules [74–76] that have an electrostatic nature,

the NQR parameter would be strongly sensitive to the electric arrangement around nuclei with $I > (1/2)$.

With this knowledge about the NQR method and the fact that the NQR parameters η and C_Q can be measured experimentally [69,77], the NQR analysis suggests a reliable method for understanding the structural changes around the phase transition temperature in our system of interest. However, to our knowledge, there has been no attempt to study the phase transition of water inside SWCNTs using a quantitative NQR investigation. In the present study, the influence of temperature variations on the electric environment of a target ^{17}O was investigated by systematic NQR of the magnitude and orientation of the EFG tensor. The results of this study should improve our understanding of the origin of the phase behavior of confined water.

Using the IUPAC rules for convention [78], diagonalization of the tensor of chemical shielding σ in its PAS yields three shielding tensor principal components in the following order: $|\sigma_{33}| \geq |\sigma_{22}| \geq |\sigma_{11}|$. In this convention, the isotropic shielding constant is given by [32] (details provided in S1):

$$\sigma_{iso} = \frac{1}{3}(\sigma_{33} + \sigma_{22} + \sigma_{11}) \quad (5)$$

The first-order quadrupolar Hamiltonian equation for the interaction between the nuclear electric quadrupole moment and the EFG at the quadrupole nucleus may be written as follows [59]:

$$\hat{H} = \frac{eQV_{zz}}{4I(2I-1)}[(3\hat{I}_z^2 - \hat{I}^2) + \eta(\hat{I}_x^2 - \hat{I}_y^2)] \quad (6)$$

Here I is the nuclear spin, eQ is the nuclear electric quadrupole moment, and V_{zz} is the largest component of the EFG tensor. The EFG is a characteristic tensor with diagonal elements V_{ii} ($ii = xx, yy, zz \cdot |V_{zz}| > |V_{yy}| > |V_{xx}|$ and $V_{zz} + V_{yy} + V_{xx} = 0$) in the PAS. The symmetry of this tensor is indicated by the asymmetry parameter η [59]:

$$\eta = \frac{|V_{yy} - V_{xx}|}{|V_{zz}|} \quad 0(\text{axial symmetry}) \leq \eta \leq 1 \quad (7)$$

In addition, the product of the principal component of the EFG tensor along the Z coordinate axis, V_{zz} to eQ is another NQR parameter, named the quadrupolar coupling constant C_Q, to determine the quadrupole interactions in MHz and kHz for oxygen and hydrogen atoms, respectively.

$$C_Q = \frac{eQV_{zz}}{h} \quad (8)$$

In the above equation, e is the elementary charge, and h is the Planck constant [69].

The orientation of the EFG tensor could be characterized by Euler angles (α, β and γ), which represent three composed rotations that move an EFG tensor from the principal axis frame to the molecular frame (Fig. 4). The composed rotation matrix $R(\alpha, \beta, \gamma)$ is shown in S2.

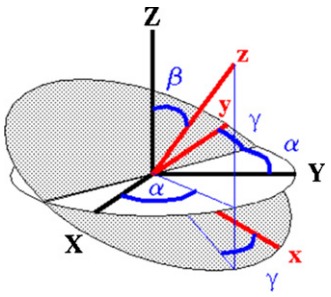

Fig. 4. Schematic representation of the orientation of the EFG tensor by Euler angles (α, β and γ), which represent three composed rotations that move an EFG tensor from the principal axis frame to the molecular frame.

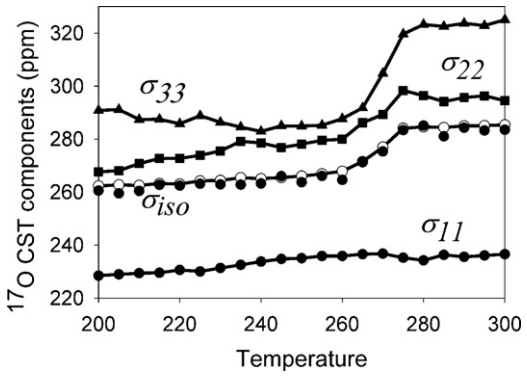

Fig. 5. The temperature dependence of isotropic chemical shielding σ_{iso} (filled circles), σ_{iso} using the PW91 method (open circles), chemical shielding tensor component σ_{11} (filled diamonds), σ_{22} (filled squares) and σ_{33} (filled triangles) for the ^{17}O atom in the water molecule in the inner side of the (9,9) SWCNT in ppm.

In this section, we attempt to scrutinize the ^{17}O EFG tensor in association with the ^{17}O chemical shielding tensor parameters of the target water molecule inside a (9,9) SWCNT. It is important to point out that because a modeled structure of the water cluster inside a carbon nanotube is taken into account, it is predicted that the calculated results would not be in agreement with the quantities that were evaluated by experimental devices, but the trends of chemical shielding and the EFG tensor with temperature variations will clarify the general behavior of the electric environment neighboring the ^{17}O atom during the phase transition. Fig. 5 shows the temperature dependence of the chemical shielding tensor for the ^{17}O atom in the water molecule on the inner side of a (9,9) SWCNT. The isotropic chemical shielding σ_{iso} and the σ_{33} and σ_{22} components of this tensor increase steadily whenever $T < T_c$. However, σ_{iso} demonstrates an irregular increase of approximately 16 ppm at approximately 10–15 K near T_c. The behavior of the chemical shielding tensor within a temperature range from 200 K to 300 K is not identical to the behavior that is expected from the structural changes in the water cluster in a single phase. This behavior is characteristic of almost every type of matter at its phase transition temperature [79,80] and strongly suggests that the chemical structure of water molecules at low temperatures must involve explicit development in the hydrogen-bonding network from 300 K to 200 K. By contrast, the σ_{11} component of the chemical shielding tensor does not show a significant sensitivity to different temperatures. This behavior may be in agreement with the fact that this element of chemical shielding is the smallest element, and its value cannot change as much as the other elements of this tensor. However, the irregular increase of σ_{iso} for the ^{17}O atom may be rationalized by considering that the electric dipole field of the hydrogen bond has an impact on oxygen atom shielding. It should be stated that repeating the calculations by another DFT method, such as PW91, could not significantly change the trends of the NMR properties of the systems, as shown in Fig. 5 and S3.

The sudden change in the ^{17}O chemical shielding tensor at T_c confirms that the transition phase mechanism includes an anomalous reorientation of the electron cloud as a result of hydrogen bonding in the water structure, which might result from the disrupted hydrogen bond network in the ice nanotube as a result of the confinement.

To confirm what have been illustrated previously, we will emphasize the effects of temperature changes on the ^{17}O EFG tensor.

Because the main goal of NQR spectroscopy is to study the interaction between the electric quadrupole moment and the EFG tensors, it would be beneficial to obtain specific information about the orientation of the ^{17}O EFG tensor to understand the source

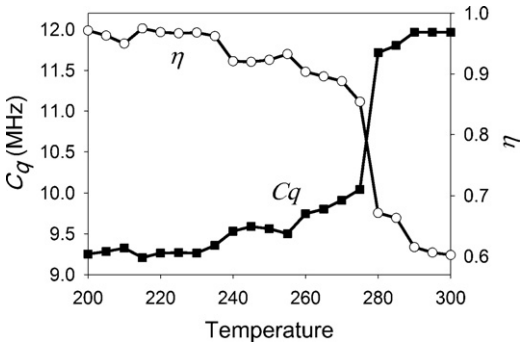

Fig. 6. Right vertical axis: the quadrupolar coupling constant, C_Q (MHz) against temperature from 200 K to 300 K for the target ^{17}O atom (filled squares). Left vertical axis: the calculated ^{17}O EFG tensor asymmetry parameter η for a range of temperatures between 200 K and 300 K (open circles).

of the ^{17}O NQR parameters. In Fig. 6, the ^{17}O EFG tensor asymmetry parameter η (right vertical axis) is increased by lowering the temperature as a consequence of constructing more hydrogen bonds and strengthening the present bonds for the target ^{17}O atom at lower temperatures. Additionally, the asymmetry parameter η increased (approximately $\Delta\eta = 0.18$) near 275 K, illustrating that water structure experiences a first-order type phase transition at this temperature. These results could signify that the V_{xx} and V_{yy} components of the EFG tensor are dramatically changed by H-bonding interactions that influence the electronic configuration around the ^{17}O nuclei. This result demonstrates the occurrence of a first-order phase transition and the reorientation of the EFG tensor in water clusters inside SWCNT could be recognized by an NQR asymmetry parameter jump following a cooling process. The use of PW91 for the NQR calculations did not change our trends of interest, as shown in S4.

The reorientation of the EFG tensor could also be studied by Euler angles. Euler angles are predicted to undergo distinct effects during the phase transition from a liquid-like state to a solid-like state (ice nanotube). In Table 1, the degree of sensitivity of the ^{17}O EFG tensor orientation to the hydrogen bonding is visualized via Euler angles (α, β, γ) of the EFG tensor at two sample temperatures, 200 K and 295 K, which are representative of temperatures before and after the phase transition, respectively. As shown in Table 1, the β angle undergoes a slight increase ($\Delta\beta$ = 14.5) from the liquid-like structure at 290 K to the ice nanotube at 200 K, while the other Euler angles, α and γ, undergo much greater changes ($\Delta\alpha$ = 22.7 and $\Delta\gamma$ = 27.1). These results suggest that the formation of hydrogen bonding in the water molecule in the confining environment is able to reorient the ^{17}O EFG tensor, similar to the effect on water molecules in other environments [81]. The dissimilarity in magnitude of these angles suggests the existence of a new type of hydrogen bonding in this system compared to bulk water. Accordingly, two different kinds of hydrogen bonding in the inter- and intra-ring positions for the ^{17}O atom can easily be distinguished by the Euler angle parameters of the EFG tensor in this atom. This study represents the first time that a balanced interrelationship between the special arrangement of the electric field gradient around an ^{17}O atom and the inter-ring and intra-ring hydrogen bonding for this atom are evaluated quantitatively.

The effects of decreasing temperature on hydrogen bonding in the water structure of interest was also studied by sketching the graph of the quadrupolar coupling constant C_Q against temperatures from 200 K to 300 K (Fig. 6, left vertical axis). This figure shows that with decreasing temperatures, C_Q values abruptly fall near T_c = 275 K ($\Delta C_Q = 1.67$ MHz). C_Q in Fig. 6 is strongly affected by the neighborhoods of the hydrogen bond donors. As demonstrated by Eq. (8), the sudden change in C_Q is related to a sharp decrease in V_{zz} as a result of reducing the surrounding electron clouds during the formation of stronger hydrogen bonding at the phase transition temperature T_c [32]. This result suggests that the first-order phase transition in water confinement inside SWCNTs strongly contributes to the electronic character of each atom in this structure. This study represents the first time that the hydrogen-bonding construction during the phase transition in confined water inside SWCNTs was inspected to determine the nature of the formation of ice nanotubes inside SWCNTs by an NQR study.

As final supporting information in the NQR and NMR analyses, a comparison is made in Tables 1 and 2 to emphasize the irregularity and unitary nature of the ice nanotube phase in comparison with other water clusters, including a water cyclic hexamer (as a unit cell of a hexagonal ice nanotube), ice crystal Ih and liquid water. The structure of an ice crystal Ih in Table 1 is given from Ref. [82], and the reported parameters for this structure in this table are calculated for a truncated structure, which is exactly fitted into a five ring (9,9) SWCNT to provide a more reliable comparison with an ice nanotube. In these tables, the ^{17}O and ^{1}H chemical shifts (δ_{iso}) and the ^{17}O and ^{2}H (**D**) quadrupole coupling constants (C_Q), asymmetry parameters of the ^{17}O and ^{2}H (**D**) atoms QC tensor (η) and Euler angles (α, β, γ) for ^{17}O nuclei are presented as experimentally observable parameters. The chemical shifts are defined as the differences between the shielding constants of the water clusters of interest and the shielding constant of the water monomer as a reference value ($\delta_{iso} = \sigma_{monomer} - \sigma_{complex}$) [57].

A simple analogy between the C_Q and η parameters for the water clusters in Table 1 shows that an ^{17}O atom in a confining structure such as an ice nanotube or water cyclic hexamer has smaller quadrupolar coupling constants and larger asymmetry parameters than those of liquid water and confined water clusters. The similarity between the NQR parameters for cyclic hexamers and ice

Table 1
Summary of measured and computed results of nuclear magnetic shielding (σ_{iso}) in ppm, chemical shift constant (δ_{iso})[a] in ppm and quadrupole coupling tensor (QC tensor) parameters, including quadrupole coupling constant (C_Q) in MHz, asymmetry parameter (η) and Euler angles (α, β, γ) in degree for oxygen ^{17}O nuclei in a water cyclic hexamer, Ice nanotube, Ice crystal Ih and liquid water. The values in parentheses are calculated using the PW91 method.

Structures	σ_{iso}	δ_{iso}	C_Q	η	α	β	γ
Ice crystal Ih	257.0[b] (253.993)	52.70[b] (50.307)	6.60[b] (6.64), 6.66[c]	0.97[b] (0.90), 0.93[c]	5.58[b]	98.03[b]	98.18[b]
Ice nanotube (200 K)[b]	262.34 (260.044)	47.36 (44.256)	9.25 (8.88)	0.89 (0.74)	55.01	41.39	37.90
Water cyclic hexamer[b]	286.39 (282.152)	23.31 (22.148)	9.30 (8.8)	0.80 (0.7)	44.89	31.54	22.76
Confined water (295 K)[b]	284.36 (278.399)	25.34 (25.901)	10.48 (9.86)	0.66 (0.59)	32.27	26.91	10.82
Liquid water	268.5[d]	41.20[d]	7.77[d], 8.00[e]	0.79[d], 0.75[f]	–	–	–

[a] The chemical shift is the difference between the shielding constant of the water clusters of interest and the shielding constant of the water monomer ($\sigma_{monomer}$ = 309.70 (304.3) ppm) as a reference value ($\delta_{iso} = \sigma_{monomer} - \sigma_{complex}$).
[b] Calculated value in the present study using the B3LYP method. The values in parentheses are calculated using the PW91 method.
[c] Experimental value given from Ref. [83].
[d] Calculated value using the B3LYP method given from Ref. [82].
[e] Experimental value given from Ref. [84].
[f] Experimental value at 300 K given from Ref. [85].

Table 2
Summary of measured and computed results of nuclear magnetic shielding (σ_{iso}) in ppm, chemical shift constant (δ_{iso})[a] in ppm for ^{1}H nuclei, and quadrupole coupling tensor (QC tensor) parameters, including quadrupole coupling constant (C_Q) in kHz and asymmetry parameter (η) for ^{2}H nuclei (D) in a water cyclic hexamer, Ice nanotube, Ice crystal Ih and liquid water.

Structures	σ_{iso}	δ_{iso}	C_Q	η
Ice crystal Ih	22.13[b]	7.97[b]	215.10[b], 214.30[c]	0.164[b], 0.16[c]
Ice nanotube (200 K)[b]	23.31 (24.01)[d]	6.79 (6.09)[d]	237.87 (243.77)[d]	0.158 (0.145)[d]
Water cyclic hexamer[b]	27.37 (26.66)[d]	2.73 (3.44)[d]	222 (278.09)[d]	0.154 (0.111)[d]
Confined water (295 K)[b]	25.49	4.61	245.03	0.141
Liquid water	24.80[e]	5.30[e]	254[c]	0.135[e]

[a] The chemical shift of ^{2}H (**D**) nuclei is the difference between the shielding constant of the water clusters of interest and the shielding constant of the water monomer ($\sigma_{monomer}$ = 30.1 ppm) as a reference value ($\delta_{iso} = \sigma_{monomer} - \sigma_{complex}$).
[b] Calculated value in the present study using the B3LYP method.
[c] Experimental value given from Ref. [86].
[d] The numbers out of the parentheses are related to the out-of-plane hydrogen atoms (inter-ring) in a water cyclic hexamer and ice nanotube and the numbers in the parentheses are related to in-plane atoms (intra-ring).
[e] Calculated value using the B3LYP method given from Ref. [81].

nanotubes and the differences between these parameters and the NQR parameters for ice Ih show that there is a disparity in the nature of the hydrogen bonding network in ice nanotubes and ice Ih structures. This finding could be related to the two different kinds of hydrogen bonds in ice nanotubes, with one kind weaker than the other, which makes the hydrogen-bonding network more similar to a cyclic hexamer than to an ice Ih.

The ^{17}O atom in an ice Ih with a specific hexagonal crystallography [83] has the strongest hydrogen bond, which could be detected by the largest value of asymmetry parameter (η) and the smallest quadrupole coupling constants (C_Q) in Table 1. These calculated values of C_Q and η are in a very good agreement with experimental results. These findings could be demonstrated by comparing the Euler angles as a representative of the orientation of the QC tensor components related to the molecular frame. In a nanoscale confining environment such as an ice nanotube, the tendency of water molecules to have the most hydrogen bonding leads to a remarkable reorientation of the ^{17}O electron cloud related to the molecular frame, which leads to the large Euler angle values compared to liquid water or confined water clusters. In ice crystal Ih, the Euler angles have noticeable values in just two directions, which could be related to the specific method of truncating that is utilized here to make the most similar ice crystal Ih to an ice nanotube cluster. These results suggest that the orientation of the electric field gradient tensor, as a second-rank characteristic of the ^{17}O atom, aids in our understanding the orientation of the electronic structure and underlying mechanism of phase transition phenomena in nanoscale systems.

Table 1 shows that the ^{17}O chemical shifts δ_{iso} (quickly reflecting their electronic environment) decrease when the ^{17}O could not have all allowed hydrogen bonding (ice rule) [83] due to the ring strain (water cyclic hexamer) or confining geometry (ice nanotube). In addition, cooperative hydrogen bonding in an ice nanotube increases the chemical shift with respect to the ^{17}O δ_{iso} value for a water cyclic hexamer. The deviation in the ^{17}O δ_{iso} value in liquid water from that expected from the confining effects could be related to our use of a different basis set (aug-cc-pVDZ) in the NMR calculation in Ref. [84] for this structure. It could be concluded from the experimentally observable NQR and NMR parameters that the confinement of water molecules in nanoscale environments causes the QC tensor to be rotated along the Euler angle to reduce its largest component, V_{zz} and increase its components in other directions. In addition, confinements reduce the chemical shielding constants of the ^{17}O atom because of the formation of a different type of hydrogen bonding network. This considerable result could be developed to use the QC and CS tensor parameters to provide reliable information about the spatial orientation of the hydrogen bonding network in confining nanoscale surroundings. The confinement effect could be observed by examining the considerable disparity in the NQR and NMR parameters between confined water at 295 K and liquid water or between ice nanotubes and ice Ih. As shown in Table 1, the calculated values with the PW91 method (values in parentheses) show similar trends. In addition, we calculated some of the results in Table 1 with the omega B97XD dispersion correction, as shown in S5.

The ^{2}H (**D**) NQR and ^{1}H NMR parameters in Table 2 are in good agreement with the results for ^{17}O nuclei, so the findings in this table provide clear evidence for the existence of two kinds of hydrogen bonding in an ice Ih structure. Here, the intra-ring H-bond in an ice nanotube has NQR and NMR parameters that are more similar to the ice Ih, while the hydrogen atom that contributes to inter-ring H-bonding has dissimilar values.

In this section, the NQR/NMR analyses support the NBO data for the phase transition phenomena and show that this phase transition consists of a significant change in the electronic structure of water molecules during an order-disorder phase transition.

4. Conclusions

The first-order phase transition of water confined in SWCNTs on cooling exhibits attractive challenges in the interpretation of its underlying chemical mechanism. In this study, we performed a series of molecular dynamic simulations to study the first-order phase transition phenomena in these systems. Here, for the first time, the strong temperature dependence of oxygen atom distributions suggests that the effectual management of the water structure inside SWCNT was identified using atomic localization. Then, the specific geometry of the confined water network inside a (9,9) SWCNT at each temperature between 200 K and 300 K was found by averaging randomly selected snapshot configurations to carry out further ab initio calculations. The NBO analysis showed that water molecules in confining structures exhibit exceptional intermolecular charge transfer during phase transition phenomena. In addition, it was found that inter-ring H-bonds in a hexagonal ice nanotube were weaker than the intra-ring bonds (nearly bulk-like) because of their unusual orientation. This finding is very important for modern chemistry because an imperfect simple model yields a good deal of information about a complex phenomenon when it is interpreted in terms of a simple NBO analysis that is in agreement with experimental data. This study also demonstrated that the main components and isotropic part of a magnetic shielding tensor can quickly respond to the electronic rearrangement and hydrogen bonding formation around the target oxygen atom during the phase transition by an abrupt change in its value. In agreement with ^{17}O NMR studies, ^{17}O NQR asymmetry, η, nuclear quadrupole resonance and C_Q parameters show very good correlations with phase transition studies that have been reported previously using other techniques. This result means that the electronic and nuclear

charge distribution surrounding the selected nucleus present a noticeable susceptibility to structural modifications through a first-order phase transition. We also demonstrated that the orientation of an EFG tensor is susceptible to the direction, strength and number of hydrogen bonds of the target oxygen atom at each specific temperature. Very good agreement between the NBO, NQR and NMR parameters was shown in this study. These results support the use of ^{17}O NQR and NMR analyses to verify sudden changes in H-bonding networks in nanoscale water confinement structures during the phase transition. In addition, through a comparison with other types of water clusters, we show that confinement decreases the quadrupolar coupling constant, increases the asymmetry parameter of water molecules and decreases the chemical shielding constants because of the reorientation of the electronic molecular structure as a result of alterations in the hydrogen bonding network.

Overall, the results of the present study represent a starting point to improve an exact tactic for determining a first-order phase transition in nanoscale water structures inside SWCNTs via NMR, especially NQR spectroscopy. Here, we propose a new route to deal with complicated phase transition behaviors in confining systems by understanding their electronic structural configurations. We remark on the prospective applications of confined water in SWCNTs at different temperatures for manufacturing nanoscale electronic and ferroelectric devices and optical nanosensors.

Appendix A. Supplementary data

Supplementary data associated with this article can be found, in the online version, at http://dx.doi.org/10.1016/j.jmgm.2012.05.009.

References

[1] M. Weik, U. Lehnert, G. Zaccai, Liquid-like water confined in stacks of biological membranes at 200 K and its relation to protein dynamics, Biophysical Journal 89 (2005) 3639–3646.
[2] A. Kalra, S. Garde, G. Hummer, Osmotic water transport through carbon nanotube membranes, Proceedings of the National Academy of Sciences of the United States of America 100 (2003) 10175–10180.
[3] K. Murata, K. Mitsuoka, T. Hirai, T. Walz, P. Agre, J.B. Heymann, A. Engel, Y. Fujiyoshi, Structural determinants of water permeation through aquaporin-1, Nature 407 (2000) 599–605.
[4] D. Mattia, Y. Gogotsi, Review: static and dynamic behavior of liquids inside carbon nanotubes, Microfluidics and Nanofluidics 5 (2008) 289–305.
[5] A. Alexiadis, S. Kassinos, Molecular simulation of water in carbon nanotubes, Chemical Reviews 108 (2008) 5014–5034.
[6] Y. Hamada, K. Koga, H. Tanaka, Phase equilibria and interfacial tension of fluids confined in narrow pores, Journal of Chemical Physics 127 (2007) 084908–084916.
[7] O. Beckstein, P.C. Biggin, M.S.P. Sansom, A hydrophobic gating mechanism for nanopores, Journal of Physical Chemistry B 105 (2001) 12902–12905.
[8] P. Gallo, Glass transition and layering effects in confined water: a computer simulation study, Journal of Chemical Physics 113 (2000) 11324–11335.
[9] M.C. Gordillo, J. Martí, High temperature behavior of water inside flat graphite nanochannels, Physical Review B: Condensed Matter 75 (2007) 085406–085410.
[10] T. Ezzat Keshavarzi, F. Sedaghat, G. Mansoori, Behavior of confined fluids in nanoslit pores: the normal pressure tensor, Microfluidics and Nanofluidics 8 (2010) 97–104.
[11] I. Brovchenko, A. Geiger, A. Oleinikova, Water in nanopores. II. The liquid–vapour phase transition near hydrophobic surfaces, Journal of Physics: Condensed Matter 16 (2004) S5345–S5370.
[12] T. Kurita, S. Okada, A. Oshiyama, Energetics of ice nanotubes and their encapsulation in carbon nanotubes from density-functional theory, Physical Review B: Condensed Matter 75 (2007) 205424–205431.
[13] E. Keshavarzi, M. Kamalvand, Energy effects on the structure and thermodynamic properties of nanoconfined fluids (a density functional theory study), Journal of Physical Chemistry B 113 (2009) 5493–5499.
[14] F. Mikami, K. Matsuda, H. Kataura, Y. Maniwa, Dielectric properties of water inside single-walled carbon nanotubes, ACS Nano 3 (2009) 1279–1287.
[15] A.I. Kolesnikov, J.-M. Zanotti, C.-K. Loong, P. Thiyagarajan, A.P. Moravsky, R.O. Loutfy, C.J. Burnham, Anomalously soft dynamics of water in a nanotube: a revelation of nanoscale confinement, Physical Review Letters 93 (2004) 035503–035506.
[16] O. Byl, J.-C. Liu, Y. Wang, W.-L. Yim, J.K. Johnson, J.T. Yates, Unusual hydrogen bonding in water-filled carbon nanotubes, Journal of the American Chemical Society 128 (2006) 12090–12097.
[17] W. Wenseleers, S. Cambré, J. Čulin, A. Bouwen, E. Goovaerts, Effect of water filling on the electronic and vibrational resonances of carbon nanotubes: characterizing tube opening by Raman spectroscopy, Advanced Materials 19 (2007) 2274–2278.
[18] Y. Maniwa, H. Kataura, M. Abe, A. Udaka, S. Suzuki, Y. Achiba, H. Kira, K. Matsuda, H. Kadowaki, Y. Okabe, Ordered water inside carbon nanotubes: formation of pentagonal to octagonal ice-nanotubes, Chemical Physics Letters 401 (2005) 534–538.
[19] Q. Yuan, Y.-P. Zhao, Hydroelectric voltage generation based on water-filled single-walled carbon nanotubes, Journal of the American Chemical Society 131 (2009) 6374–6376.
[20] K. Koga, G.T. Gao, H. Tanaka, X.C. Zeng, Formation of ordered ice nanotubes inside carbon nanotubes, Nature 412 (2001) 802–805.
[21] K. Koga, Freezing in one-dimensional liquids, Journal of Chemical Physics 118 (2003) 7973–7980.
[22] S. Han, M.Y. Choi, P. Kumar, H.E. Stanley, Phase transitions in confined water nanofilms, Nature Physics 6 (2010) 685–689.
[23] Z. Fu, Y. Luo, J. Ma, G. Wei, Phase transition of nanotube-confined water driven by electric field, Journal of Chemical Physics 134 (2011) 154507–154512.
[24] D. Takaiwa, I. Hatano, K. Koga, H. Tanaka, Phase diagram of water in carbon nanotubes, Proceedings of the National Academy of Sciences of the United States of America 105 (2008) 39–43.
[25] B.K. Agrawal, V. Singh, A. Pathak, R. Srivastava, Ab initio study of ice nanotubes in isolation or inside single-walled carbon nanotubes, Physical Review B: Condensed Matter 75 (2007) 195420–195428.
[26] A. Alexiadis, S. Kassinos, Influence of water model and nanotube rigidity on the density of water in carbon nanotubes, Chemical Engineering Science 63 (2008) 2793–2797.
[27] N. Perez-Hernandez, T.Q. Luong, C. Perez, J.D. Martin, M. Havenith, Pore size dependent dynamics of confined water probed by FIR spectroscopy, Physical Chemistry Chemical Physics 12 (2010) 6928–6932.
[28] E. Mamontov, C.J. Burnham, S.H. Chen, A.P. Moravsky, C.K. Loong, N.R. De Souza, A.I. Kolesnikov, Dynamics of water confined in single- and double-wall carbon nanotubes, Journal of Chemical Physics 124 (2006) 194703–194708.
[29] H. Kyakuno, Confined water inside single-walled carbon nanotubes: global phase diagram and effect of finite length, Journal of Chemical Physics 134 (2011) 244501–244514.
[30] F. Weinhold, C.R. Landis, Valency and Bonding: A Natural Bond Orbital Donor–Acceptor Perspective, Cambridge University Press, Cambridge, 2005.
[31] A.E. Reed, L.A. Curtiss, F. Weinhold, Intermolecular interactions from a natural bond orbital, donor–acceptor viewpoint, Chemical Reviews 88 (1988) 899–926.
[32] M.H. Levitt, Spin Dynamics: Basics of Nuclear Magnetic Resonance, John Wiley & Sons, New York, 2001.
[33] R.S. Drago, Physical Methods in Chemistry, Academic Press Inc., London and New York, 1977.
[34] W. Smith, T.R. Forester, I.T. Todorov, The DL_POLY Classic User Manual, Daresbury Laboratory, United Kingdom, 2010.
[35] H.J.C. Berendsen, J.R. Grigera, T.P. Straatsma, The missing term in effective pair potentials, Journal of Physical Chemistry 91 (1987) 6269–6271.
[36] S. Maruyama, Handbook of Numerical Heat Transfer, Wiley, New York, 2006.
[37] M.P. Allen, D.J. Tildesley, Computer Simulation of Liquids, Oxford University Press, Clarendon, 1989.
[38] S.J. Weiner, P.A. Kollman, D.T. Nguyen, D.A. Case, An all atom force field for simulations of proteins and nucleic acids, Journal of Computational Chemistry 7 (1986) 230–252.
[39] J.H. Walther, R. Jaffe, T. Halicioglu, P. Koumoutsakos, Carbon nanotubes in water: structural characteristics and energetics, Journal of Physical Chemistry B 105 (2001) 9980–9987.
[40] R.B. Best, G. Hummer, Reaction coordinates and rates from transition paths, Proceedings of the National Academy of Sciences of the United States of America 102 (2005) 6732–6737.
[41] H. Berendsen, Molecular dynamics with coupling to an external bath, Journal of Chemical Physics 81 (1984) 3684–3690.
[42] J.M. Haile, Molecular Dynamics Simulation: Elementary Methods, Wiley, Chichester, 1992.
[43] W. Koch, M.C. Holthausen, A Chemist's Guide to Density Functional Theory, Wiley-VCH, Weinheim, 2001.
[44] A. Becke, Density functional thermochemistry. III. The role of exact exchange, Journal of Chemical Physics 98 (1993) 5648–5652.
[45] P.J. Stephens, F.J. Devlin, C.F. Chabalowski, M.J. Frisch, Ab initio calculation of vibrational absorption and circular dichroism spectra using density functional force fields, Journal of Physical Chemistry 98 (1994) 11623–11627.
[46] M.J. Frisch, G.W. Trucks, H.B. Schlegel, G.E. Scuseria, M.A. Robb, J.R. Cheeseman, V.G. Zakrzewski, J.A. Montgomery Jr., R.E. Stratmann, J. Burant, C.S. Dapprich, J.M. Millam, A.D. Daniels, K.N. Kudin, M.C. Strain, O. Farkas, J. Tomasi, V. Barone, M. Cossi, R. Cammi, B. Mennucci, C. Pomelli, C. Adamo, S. Clifford, J. Ochterski, G.A. Petersson, P.Y. Ayala, Q. Cui, K. Morokuma, D.K. Malick, A.D. Rabuck, K. Raghavachari, J.B. Foresman, J. Cioslowski, J.V. Ortiz, B.B. Stefanov, G. Liu, A. Liashenko, P. Piskorz, I. Komaromi, R. Gomperts, R.L. Martin, T.K.D.J. Fox, M.A. Al-Laham, C.Y. Peng, A. Nanayakkara, C. Gonzalez, M. Challacombe, P.M.W. Gill, B. Johnson, W. Chen, M.W. Wong, J.L. Andres, C. Gonzalez, M. Head-Gordon, S. Replogle, J.A. Pople, Gaussian 98, Revision A, 6th ed., Gaussian Inc., Pittsburgh, PA, 1998.

[47] E.D. Glendening, A.E. Reed, J.E. Carpenter, F. Weinhold, Nbo Version 3.1.
[48] W. Klopper, J.G.C.M. van Duijneveldt-van de Rijdt, F.B. van Duijneveldt, Computational determination of equilibrium geometry and dissociation energy of the water dimer, Physical Chemistry Chemical Physics 2 (2000) 2227–2234.
[49] A. Alexiadis, S. Kassinos, The density of water in carbon nanotubes, Chemical Engineering Science 63 (2008) 2047–2056.
[50] I. Hanasaki, T. Yonebayashi, S. Kawano, Molecular dynamics of a water jet from a carbon nanotube, Physical Review E – Statistical Physics, Plasmas, Fluids, and Related Interdisciplinary Topics 79 (2009) 046307–046313.
[51] C. Luo, W. Fa, J. Zhou, J. Dong, X.C. Zeng, Ferroelectric ordering in ice nanotubes confined in carbon nanotubes, Nano Letters 8 (2008) 2607–2612.
[52] J.A. Thomas, Density, distribution, and orientation of water molecules inside and outside carbon nanotubes, Journal of Chemical Physics 128 (2008) 084715–084720.
[53] D. Frenkel, B. Smit, Understanding Molecular Simulation: From Algorithms to Applications, Academic Press, Florida, 2002.
[54] J. Bai, Ab initio studies of quasi-one-dimensional pentagon and hexagon ice nanotubes, Journal of Chemical Physics 118 (2003) 3913–3916.
[55] M.S. Dresselhaus, G. Dresselhaus, P. Avouris, Carbon Nanotubes: Synthesis, Structure, Properties, and Applications, Springer, New York, 2001.
[56] H.A. Bent, An appraisal of valence-bond structures and hybridization in compounds of the first-row elements, Chemical Reviews 61 (1961) 275–311.
[57] H. Cybulski, J. Sadlej, On the calculations of the nuclear shielding constants in small water clusters, Chemical Physics 323 (2006) 218–230.
[58] J. Holt, Methods for probing water at the nanoscale, Microfluidics and Nanofluidics 5 (2008) 425–442.
[59] M.J. Duer, Solid-state NMR Spectroscopy: Principles and Applications, Blackwell Science Ltd., London, 2002.
[60] A. Rigamonti, NMR–NQR studies of structural phase transitions, Advances in Physics 33 (1984) 115–191.
[61] K. Matsuda, T. Hibi, H. Kadowaki, H. Kataura, Y. Maniwa, Water dynamics inside single-wall carbon nanotubes: NMR observations, Physical Review B: Condensed Matter 74 (2006), 073415-1–073415-4.
[62] W. Sekhaneh, M. Kotecha, U. Dettlaff-Weglikowska, W.S. Veeman, High resolution NMR of water absorbed in single-wall carbon nanotubes, Chemical Physics Letters 428 (2006) 143–147.
[63] S. Ghosh, K.V. Ramanathan, A.K. Sood, Water at nanoscale confined in single-walled carbon nanotubes studied by NMR, Europhysics Letters 65 (2004) 678–684.
[64] N.A. Besley, NMR chemical shifts of molecules encapsulated in single walled carbon nanotubes, Journal of Chemical Physics 128 (2008) 101102–101105.
[65] P. Huang, E. Schwegler, G. Galli, Water confined in carbon nanotubes: magnetic response and proton chemical shieldings, Journal of Physical Chemistry C 113 (2009) 8696–8700.
[66] M. Vogel, NMR studies on simple liquids in confinement, European Physical Journal Special Topics 189 (2010) 47–64.
[67] B. Nogaj, Hydrogen-bond theories and models based on nuclear quadrupole resonance spectroscopy studies, Journal of Physical Chemistry 91 (1987) 5863–5869.
[68] L.G. Butler, C.P. Cheng, T.L. Brown, Oxygen-17 nuclear quadrupole double resonance. 6. Effects of hydrogen bonding, Journal of Physical Chemistry 85 (1981) 2738–2740.
[69] E.A. Lucken, Nuclear Quadrupole Coupling Constant, Academic Press, London, 1969.
[70] S. Javadian, R. Araghi, A DFT study of the ^{67}Zn, ^{14}N and ^{2}H electric field gradient tensors in zinc(ii)–4-meim complexes and extrapolation to superoxide dismutase, Journal of Molecular Graphics and Modelling 27 (2009) 620–627.
[71] K. Yamada, T. Shimizu, T. Yamazaki, S. Ohki, Determination of the orientations for the ^{17}O NMR tensors in a polycrystalline L-alanine hydrochloride, Solid State Nuclear Magnetic Resonance 33 (2008) 88–94.
[72] M.D. Esrafili, H. Behzadi, N.L. Hadipour, Density functional theory study of N—H···O, O—H···O and C—H···O hydrogen-bonding effects on the ^{14}N and ^{2}H nuclear quadrupole coupling tensors of n-acetyl-valine, Biophysical Chemistry 133 (2008) 11–18.
[73] S. Khodaei, N.L. Hadipour, M.R. Kasaai, Theoretical investigation of hydrogen bonding effects on oxygen, nitrogen, and hydrogen chemical shielding and electric field gradient tensors of chitosan/HI salt, Carbohydrate Research 342 (2007) 2396–2403.
[74] I. Hanasaki, Hydrogen bond dynamics and microscopic structure of confined water inside carbon nanotubes, Journal of Chemical Physics 124 (2006) 174714–174722.
[75] N.S. Dalal, O. Gunaydin-Sen, R. Fu, R. Achey, K.L. Pierce, High resolution NMR evidence for displacive behavior in hydrogen-bonded ferroelectrics and antiferroelectrics, Ferroelectrics 337 (2006) 3–12.
[76] M.D. Fayer, N.E. Levinger, Analysis of water in confined geometries and at interfaces, Annual Review of Analytical Chemistry 3 (2010) 89–107.
[77] G. Wu, P. Mason, X. Mo, V. Terskikh, Experimental and computational characterization of the ^{17}O quadrupole coupling and magnetic shielding tensors for p-nitrobenzaldehyde and formaldehyde, Journal of Physical Chemistry A 112 (2008) 1024–1032.
[78] J. Mason, Conventions for the reporting of nuclear magnetic shielding (or shift) tensors suggested by participants in the NATO ARW on NMR shielding constants at the University of Maryland, College Park, July 1992, Solid State Nuclear Magnetic Resonance 2 (1993) 285–288.
[79] F. Mallamace1, M. Broccio, C. Corsaro, A. Faraone, L. Liu, C.Y. Mou, S.H. Chen, Dynamical properties of confined supercooled water: an NMR study, Journal of Physics: Condensed Matter 18 (2006) S2285–S2297.
[80] N.S. Dalal, K.L. Pierce, J. Palomar, R. Fu, Single-crystal magic-angle spinning ^{17}O NMR and theoretical studies of the antiferroelectric phase transition in squaric acid, Journal of Physical Chemistry A 107 (2003) 3471–3475.
[81] T.S. Pennanen, P. Lantto, A.J. Sillanpää, J. Vaara, Nuclear magnetic resonance chemical shifts and quadrupole couplings for different hydrogen-bonding cases occurring in liquid water: a computational study, Journal of Physical Chemistry A 111 (2006) 182–192.
[82] D. Eisenberg, W. Kauzmann, The Structure and Properties of Water, Oxford University Press, New York and Oxford, 1969.
[83] L. Pauling, The structure and entropy of ice and of other crystals with some randomness of atomic arrangement, Journal of the American Chemical Society 57 (1935) 2680–2684.
[84] T.S. Pennanen, J. Vaara, P. Lantto, A.J. Sillanpää, K. Laasonen, J. Jokisaari, Nuclear magnetic shielding and quadrupole coupling tensors in liquid water: a combined molecular dynamics simulation and quantum chemical study, Journal of the American Chemical Society 126 (2004) 11093–11102.
[85] H. Spiess, Oxygen-17 quadrupole coupling parameters for water in its various phases, Journal of Chemical Physics 51 (1969) 1201–1205.
[86] R.P.W.J. Struis, J. De Bleijser, J.C. Leyte, Dynamic behavior and some of the molecular properties of water molecules in pure water and in magnesium chloride solutions, Journal of Physical Chemistry 91 (1987) 1639–1645.